

Cost optimal scenarios of a future highly renewable European electricity system: Exploring the influence of weather data, cost parameters and policy constraints

D.P. Schlachtberger^{a,b,*}, T. Brown^a, M. Schäfer^b, S. Schramm^a, M. Greiner^b

^aFrankfurt Institute for Advanced Studies, 60438 Frankfurt am Main, Germany

^bDepartment of Engineering, Aarhus University, 8000 Aarhus C, Denmark

Abstract

Cost optimal scenarios derived from models of a highly renewable electricity system depend on the specific input data, cost assumptions and system constraints. We study this influence using a techno-economic optimisation model for a networked system of 30 European countries, taking into account the capacity investment and operation of wind, solar, hydroelectricity, natural gas power generation, transmission, and different storage options. We observe a considerable robustness of total system costs to the input weather data and to moderate changes in the cost assumptions. We show that flat directions in the optimisation landscape around cost-optimal configurations often allow system planners to choose between different technology options without a significant increase in total costs, for instance by replacing onshore with offshore wind power capacity in case of public acceptance issues. Exploring a range of CO₂ emission limits shows that for scenarios with moderate transmission expansion, a reduction of around 57% compared to 1990 levels is already cost optimal. For stricter CO₂ limits, power generated from gas turbines is at first replaced by generation from increasing renewable capacities. Non-hydro storage capacities are only built for low-emission scenarios, in order to provide the necessary flexibility to meet peaks in the residual load.

Keywords: energy system design, large-scale integration of renewable power generation, power transmission, CO₂ emission reduction targets

1. Introduction

In order to meet the ambitious target of reducing CO₂ emissions in the European Union by 80% to 95% in 2050 compared to 1990 values, the electricity system has to undergo a fundamental transformation [1]. Wind and solar power plants are already today both mature and cost-efficient technology options, which can be scaled up to act as the basis of a low-emission future power supply [2, 3]. The challenges presented by the temporal fluctuations in these resources can be met with low-carbon technologies such as existing hydroelectricity power plants, or with storage options like batteries or hydrogen storage, which still have significant potential for further development [4, 5, 6, 7, 8, 9]. With respect to the spatial variability of weather-dependent renewable generation, large-scale power transmission capacities play a decisive role to provide a smoothing effect and to connect generation capacity at favorable distant locations with the load centres [10, 11, 12, 13, 14, 15, 16, 17, 18].

Given the complexity of such a system, in particular with respect to the spatio-temporal patterns and correlations in the renewable generation and load time series, it is a difficult task to deduce a cost-efficient overall system layout from heuristic principles alone. As a consequence, the role of computational models is a central element in the development of policy guidelines for the design of a future low-emission energy

system [19]. For each model, choices have to be made regarding the methodological scheme and the scope of its system representation (for instance the spatial and temporal scale, or the choice of energy sectors and technology options considered in the model). The resulting diversity of system models represents a challenge for the interpretation and comparison of the corresponding results, in particular if the underlying input data or modelling details are not publicly accessible. In this context, open energy modelling promises to provide a more transparent and comprehensible scientific approach [20].

However, even for a single system model for which all input data and modelling details are transparent, the deeper understanding of the numerical results that is fundamental for robust policy advice can be hindered by the dependence of the results on the choice of the model parameters. In particular the details of the input data, the cost assumptions, and the constraints employed in the model all affect the properties of the resulting scenarios in a non-trivial way.

In this contribution we address these issues by studying in detail the influence of weather data, cost parameters and policy constraints on the properties of cost optimal scenarios of a future highly renewable electricity system taken from [15]. We show that the total system costs are only weakly affected by the choice of the input weather data or by small changes in the capital costs. The optimisation landscape is flat in many directions, which allows system planners to choose between different near optimal system configurations without a significant increase in total costs. With respect to policy constraints, the investigation

*Corresponding author

Email address: schlachtberger@fias.uni-frankfurt.de
(D.P. Schlachtberger)

Nomenclature

n	nodes (countries)	$f_{\ell,t}$	power flow
t	hours of the year	F_{ℓ}	transmission capacity
s	generation and storage technologies	$K_{n\ell}$	incidence matrix
ℓ	inter-connectors	l_{ℓ}	length of transmission line
$c_{n,s}$	fixed annualised generation and storage costs	EU	European Union
c_{ℓ}	fixed annualised line costs	H_2	molecular hydrogen
$o_{n,s}$	variable generation costs	HVAC	high-voltage alternating current
e_s	specific CO ₂ emissions	HVDC	high-voltage direct current
$d_{n,t}$	demand	NTC	net transfer capacity
$g_{n,s,t}$	generation and storage dispatch	OCGT	open-cycle gas turbines
$\bar{g}_{n,s,t}$	availability per unit of capacity	O&M	operation and maintenance
$G_{n,s}$	generation and storage capacity	PHS	pumped hydro storage
$G_{n,s}^{max}$	maximum installable capacity	PV	solar photovoltaic

of a wide range of CO₂ emission limits helps to understand the mechanisms in the cost-efficient interplay of different technology options along the pathway towards a future low-emission electricity system.

The approach taken in the present contribution goes beyond the small variations of a few selected input parameters that are commonly used in the literature to test robustness. Here we consider very large changes to input parameters to try to understand fully what role each system component plays in the cost-optimal system.

In the literature, the consideration of different input assumptions is often limited to the focus of the respective study. For instance in [15], Schlachtberger et al. focus on the role of transmission expansion for the layout and cost structure of a low-emission European electricity system. The parameter variation is then mainly limited to the constraint for the total transmission capacity as the crucial parameter of the study, but not expanded in a similar way to other model dimensions. Similarly, in [11] the authors analyse the effects of grid extensions in a renewable Europe, with a focus on the influence of the composition of the power generation in the system. The screening of parameter ranges for the renewable penetration and the mix between solar and wind is the central line of the investigation. In other cases, a sensitivity analysis of modelling results is added to the presentation of a numerical study to assess the robustness of the numerical findings. Such an analysis usually addresses only a few key parameters, but is not central to the understanding of the workings of the system. For instance in [16], the authors model a renewable-based European electricity system including storage options and concentrated solar power. Choosing different investment costs for storage, grid and backup technologies, they find that although the system composition and operation is highly dependent on these parameters, the overall system cost

is only slightly affected.

This article starts with a review of the model and the data inputs in Sec. 2. In Sec. 3 we present results on the sensitivity to different samples of weather and load data and in Sec. 4 to changes in the cost assumptions. The subsequent Sec. 5 explores the role of policy constraints, such as limits on the expansion of onshore wind, or different CO₂ limits. Finally in Sec. 6 the limitations of this study are discussed, before conclusions are drawn in Sec. 7.

2. Methods

2.1. Model

We study scenarios of a future European electricity system using the model presented in [15], which applies a linear techno-economic optimisation of total annual costs:

$$\min_{G_{n,s}, F_{\ell}, g_{n,s,t}, f_{\ell,t}} \left(\sum_{n,s} c_{n,s} G_{n,s} + \sum_{n,s,t} o_{n,s} g_{n,s,t} + \sum_{\ell} c_{\ell} F_{\ell} \right). \quad (1)$$

The indices n label the nodes of the system, which represent with one node per country the EU-28 (as of 2018) without Cyprus and Malta, but including Norway, Switzerland, Serbia, and Bosnia and Herzegovina. The system costs are composed of fixed annualised costs $c_{n,s}$ for generation and storage capacity $G_{n,s}$, variable costs $o_{n,s}$ for generation and storage dispatch $g_{n,s,t}$, and fixed annualised costs c_{ℓ} for transmission capacity F_{ℓ} . The indices s label the generation and storage technologies comprising onshore wind, offshore wind, solar PV, open cycle gas turbines (OCGT), hydrogen storage (electrolysis and fuel cells for conversion, steel tanks for storage), central batteries (lithium ion), pumped hydro storage, hydro reservoir, and run-of-river hydro generation.

The optimisation problem in Eq. (1) is subject to several constraints. Assuming an inelastic demand $d_{n,t}$ at node n and time t , the instantaneous balancing of energy supply and demand translates into the power balance constraints

$$\sum_s g_{n,s,t} - d_{n,t} = \sum_\ell K_{n\ell} f_{\ell,t} \quad \forall n, t, \quad (2)$$

where $K_{n\ell}$ is the incidence matrix of the network. Here $f_{\ell,t}$ denotes the power flow at time t on the line ℓ representing the cross-border transmission between the respective two interconnected countries in the European electricity system. The power transmission is modelled as a transport model, given the increasingly controllable nature of international connections realised as point-to-point HVDC connections or using phase-shifting transformers in the case of HVAC connections. The absolute power flows have to respect the capacity limits

$$|f_{\ell,t}| \leq F_\ell \quad \forall \ell, t, \quad (3)$$

with the system model determining the line capacities F_ℓ in its optimisation of total system costs in Eq. (1). In Ref. [15] a cap CAP_{LV} of the total transmission line capacities multiplied by their lengths was introduced,

$$\sum_\ell l_\ell \cdot F_\ell \leq CAP_{LV}, \quad (4)$$

with the influence of this constraint on system costs representing one focus of the study.

Further constraints apply to the dispatch $g_{n,s,t}$ of both conventional and renewable generators as well as the storage operation. While the conventional generators can be dispatched up to their nominal capacity $G_{n,s}$,

$$0 \leq g_{n,s,t} \leq G_{n,s} \quad \forall n, s, t, \quad (5)$$

the potential renewable generation in each installed unit of the respective generators depends on the given weather conditions:

$$0 \leq g_{n,s,t} \leq \bar{g}_{n,s,t} \cdot G_{n,s} \quad \forall n, s, t. \quad (6)$$

Here the availability $\bar{g}_{n,s,t}$ times the capacity $G_{n,s}$ gives the maximum renewable energy generation according to the weather conditions at node n and time t . Note that we assume that this potential renewable generation can always be curtailed, such that Eq. (6) describes the limits of the corresponding possible dispatch. In the following, the term ‘renewable generation’ always refers to this dispatch after curtailment. Both the conventional and the renewable dispatch, as well as the installed capacity itself are a result of the optimisation in Eq. (1), with the maximum installed renewable capacity $G_{n,s}^{max} \geq G_{n,s}$ following an assessment of the geographic potentials. For the operation of the different storage technologies, the state-of-charge has to be consistent with the charging / discharging in each hour while respecting the storage capacity, with operational losses being taken into account by corresponding efficiency parameters. The storage capacities are assumed to be proportional to the power capacities, with the ratio $h_{s,max}$ representing the time in which

a storage unit can be fully charged or discharged at maximum power. We assume $h_{s,max} = 6h$ for batteries and pumped hydro storage as short-term storage options, and $h_{s,max} = 168h$ for hydrogen as long-term storage. Standing losses in the storage units are neglected. For the full storage equations consult Ref. [15].

Given the political significance of greenhouse gas emission targets of the EU member states, the total amount of CO₂ emissions is a key characteristic of the system. Such an emission limit enters the model as a cap CAP_{CO_2} on the total emissions, implemented using the specific emissions e_s in CO₂-tonne-per-MWh of the fuel of generator type s with efficiency η_s :

$$\sum_{n,s,t} \frac{1}{\eta_s} g_{n,s,t} \cdot e_s \leq CAP_{CO_2}. \quad (7)$$

The only generators in the model with a non-zero CO₂ emission are open-cycle gas turbines with $e_s = 0.19$ tonne-CO₂/MWh_{th}, or equivalently $e_s \approx 490$ g-CO₂/kWh_{el} (see Tab. 1). For further details we refer the reader to Ref. [15].

The model was implemented in the free software energy system framework PyPSA [21].

2.2. Data

All data underlying the model reviewed in the last section is extensively described in [15]. In the following we only briefly outline this data and refer to the aforementioned publication for further details.

For each scenario the model is run over a time series comprising one or multiple years with hourly resolution. The load in each country is given by the time series provided by the transmission system operators [22, 23]. The renewable generation from onshore wind, offshore wind, and solar photovoltaic (PV) power generation are derived from historic weather data with a temporal hourly and a 40×40 km² spatial resolution. Using models for the renewable generation infrastructure, this weather data is converted into a potential wind/solar generation time series for each cell [24, 25]. By applying suitable capacity layouts, the resulting spatially-detailed potential generation data is then aggregated into generation time series on country level. These capacity layouts take into consideration the spatial distribution of the renewable resource quality inside the countries, as well as the geographical potentials considering the land use type, nature reserves, restricted areas, and likely public acceptance [14, 26, 27]. Hydroelectricity generation comprises reservoir hydro and run-of-river power plants according to the currently installed capacity, with the hourly generation following inflow time series on country level [28, 29, 30, 31]. As a conventional backup system the model can build flexible open-cycle gas turbines (OCGT) [32], whose global annual energy generation is restricted by the EU CO₂ emission limit represented by the cap CAP_{CO_2} . As possible storage technologies, the model includes pumped hydro storage (PHS), central batteries, and hydrogen (H₂) storage, with the hydro storage assumed to correspond to the currently installed capacities [6, 28]. The cost assumptions regarding all generation and storage technologies are summarised in Tab. 1. A discount rate of 7% is assumed in order to convert overnight capital costs into net present costs.

Table 1: Input parameters based on 2030 value estimates from [32] unless stated otherwise (taken from [15]).

Technology	investment (€/kW)	fixed O&M cost (€/kW/year)	variable cost (€/MWh)	lifetime (years)	efficiency (fraction)	capital cost per energy storage (€/kWh)	h_{max} (h)
onshore wind	1182	35	0.015 ^a	25	1		
offshore wind	2506	80	0.02 ^a	25	1		
solar PV	600	25	0.01 ^a	25	1		
OCGT ^b	400	15	58.4 ^c	30	0.39		
hydrogen storage ^d	555	9.2	0	20	$0.75 \cdot 0.58^e$	8.4	168
central battery (LiTi) ^d	310	9.3	0	20	$0.9 \cdot 0.9^e$	144.6	6
transmission ^f	400 €/MWkm	2%	0	40	1		
PHS	2000 ^g	20	0	80	0.75	N/A ^g	6
hydro reservoir	2000 ^g	20	0	80	0.9	N/A ^g	fixed ^h
run-of-river	3000 ^g	60	0	80	0.9		

^a The order of curtailment is determined by assuming small variable costs for renewables.

^b Open-cycle gas turbines have a CO₂ emission intensity of 0.19 CO₂-tonne/MWh_{th}.

^c This includes fuel costs of 21.6 €/MWh_{th}.

^d Budischak et al. [6].

^e The storage round-trip efficiency consists of charging and discharging efficiencies $\eta_1 \cdot \eta_2$.

^f Hagspiel et al. [33]. Costs for converter pairs of 150000€/MW and an (n-1) security factor of 1.5 are taken into account for the transmission cost assumptions (see Ref. [15] for details).

^g The installed facilities are not expanded in this model and are considered to be amortised.

^h Determined by size of existing energy storage [28, 30].

Table 2: Optimised average system costs in [€/MWh] for the allowed total interconnecting line volume of the zero, compromise, and optimal grid scenarios. Also given is the total line volume (adapted from Ref. [15])

Scenario	Zero	Comp.	Opt.
Line vol. [TWkm]	0.0	125.0	285.70
battery storage	9.9	4.5	1.7
hydrogen storage	8.1	3.4	3.1
gas	4.6	4.1	4.5
solar	26.1	14.7	9.4
onshore wind	22.3	23.4	28.6
offshore wind	10.8	11.4	7.5
transmission lines	0.0	3.6	7.6
PHS	0.3	0.3	0.3
run-of-river	1.4	1.4	1.4
reservoir hydro	0.8	0.8	0.8
Total cost	84.1	67.5	64.8

2.3. The base scenarios

As the base scenarios for the present study we choose three configurations reported in Ref. [15]. Building on consumption and generation time series for the year 2011, the system optimisation according to Eq. (1) is performed for a CO₂ cap corresponding to a reduction of 95% of European CO₂ emissions compared to 1990. Three different levels of total transmission capacity interpolate between a locally-balanced, storage-dominated system and a continental-scale, network-dominated system: The zero transmission scenario neglects any transmission capacity between the European countries, resulting in in-

dependently optimised systems for each of the European countries, with an average system cost of 84.1 €/MWh. The optimal transmission scenario does not invoke any exogenous limit to the total transmission capacity. This allows a reduction of total systems costs to 64.8 €/MWh, with a total line volume of 286 TWkm or approximately nine times the sum of today's net transfer capacities (NTCs) of 31 TWkm. The compromise transmission scenario restricts the total line volume in Eq. (4) to an intermediate value of four times today's total capacities, CAP_{LV}=125 TWkm, which already locks in a reduction of system costs to 67.5 €/MWh. The main characteristics of these three base scenarios are reviewed in Tab. 2; for further details consult Ref. [15].

3. Results I: Sensitivity to the input weather and load time series

The base scenarios presented in [15] build on time series for renewable generation potential and consumption with hourly resolution for the year 2011. Given the decisive role of weather dependent generation from wind and solar in relation to the consumption patterns for a low emission electricity system, the optimised layouts and the associated cost structures will depend on this input data. In this section we explore this sensitivity of system costs to changes in the load and renewable generation time series.

Different single historical weather years. First, the single year optimisations of the base scenarios (2011) are repeated for the weather and load data for the years 2012 to 2014. This limited

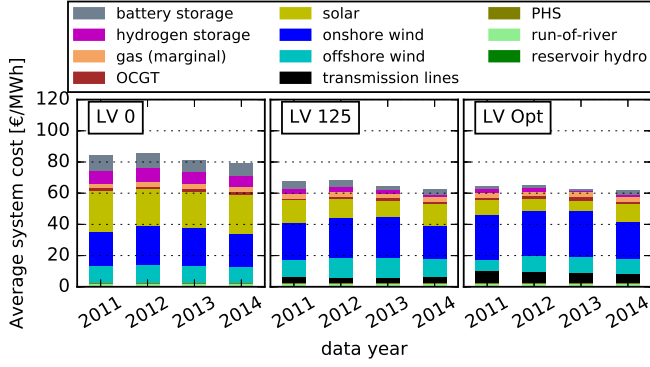


Figure 1: Composition of the average total system costs per unit of generated energy for the four different weather and demand input years 2011 to 2014 (left to right bars) for the zero, compromise, and optimal (left to right panels) transmission grid scenarios.

time frame is not further expanded due to the restricted availability of consistent load and hydro inflow datasets.

Figure 1 shows that the optimal system configuration depends to some extent on the simulated year, with the average system costs for the compromise grid volume ranging from 62.6 to 67.9 €/MWh. In order to assess the year-dependent resource quality of renewable power generation, we define the annual average capacity factor cf_s as

$$cf_s = \frac{\sum_n \langle \bar{g}_{n,s,t} \rangle_t \cdot G_{n,s}^{max}}{\sum_n G_{n,s}^{max}}, \quad (8)$$

where the temporal average $\langle \cdot \rangle_t$ is taken over all hours of the year under consideration. This measures the average amount of energy that can be produced per unit of installed capacity. To allow for a clearer comparison of the weather conditions, we choose a fixed capacity layout given by the installation potential $G_{n,s}^{max}$ for all years rather than the year-dependent layout $G_{n,s}$ resulting from the system optimisation. In Fig. 2 we display the relative changes of the values compared to the capacity factor $cf_s = 0.485, 0.233, 0.128$ for offshore wind, onshore wind, and solar obtained for the base scenarios data year 2011. The composition of the system in terms of shares of onshore wind and solar installations is largely determined by the respective capacity factors. For the weather years with capacity factor lower than in 2011, the installed capacities are also proportionately lower, and vice versa (compare Figs. 1 and 2). The size of offshore wind installations does not follow the same trend but remains relatively stable. This can be explained by the fact that offshore wind is only built in a few countries and that the average capacity factor is much higher and therefore the benefit of a smoother generation profile is more important than a slightly lower capacity factor.

The regional distribution of the generators in the compromise transmission scenario is shown in Fig. 3 and follows the expected trends. In the data year 2013, for which the solar capacity factor is lowest, the countries that are usually solar dominated such as Spain and Italy see cost optima with significant shares of onshore wind, while in 2014, when the total solar share is relatively high, there are solar installations as far north

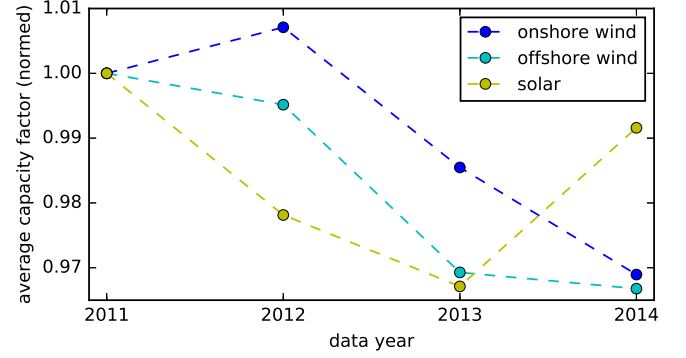


Figure 2: Average capacity factor cf_s of onshore wind (blue), offshore wind (cyan), and solar (yellow) for different weather years, normalised to $cf_s = 0.233, 0.485, 0.128$ for offshore wind, onshore wind, and solar obtained for the data year 2011. A fixed capacity layout given by the installation potential $G_{n,s}^{max}$ has been assumed for all years. The data points are marked by circles, with the dashed lines drawn as visual aids.

as Poland. The transmission capacity has to be redistributed only to a small extent to adapt to the slightly different generation capacity layouts. Note the higher total system costs in the data year 2012 compared to 2011 (1.6% / 0.65% / 0.67% for the scenario without / with moderate / with optimal transmission), despite the higher onshore wind and only marginally lower offshore wind capacity factor. This relation indicates that weather conditions corresponding to a higher capacity factor alone do not necessarily reduce the total system costs. Spatio-temporal correlations in the combined load and generation time series are also important to determine the cost optimum.

Multi-year optimisation. Instead of modelling the system for a single year of weather and load data, it can also be optimised for a longer period of continuous input data. This inclusion of a larger dataset might result in a solution that is less sensitive to changes in the input parameters due to its adaption to a potentially larger spectrum of generation and demand situations. Starting from the weather and load year 2011 considered in the base scenarios, we consider a simultaneous optimisation over one to four years of continuous data. The limitation to four years of data is founded in the restricted availability of consistent datasets and in the considerable computational demands of running multi-year optimisations [15]. Figure 4 shows that for the compromise grid scenario the average total system costs 67.1 ± 0.7 €/MWh deviate very little from the value 67.5 €/MWh of the base scenario. This result is also close to the maximum cost of the single year simulations (2012: 67.8 €/MWh), indicating that the system capacity is set by a few extreme events over the whole period. The maximum cost difference between the four year and the single year simulations is 3.5 €/MWh, a 5.5% increase from the value of the weather year 2014. In the range of the time span considered in this study, this is a lower bound for the uncertainty of a single year optimisation compared to longer-term modelling. Similar to the single year optimisations, the shares of onshore wind and solar installations in the multi-year models are proportional to the corresponding average capacity factors. However, the changes in

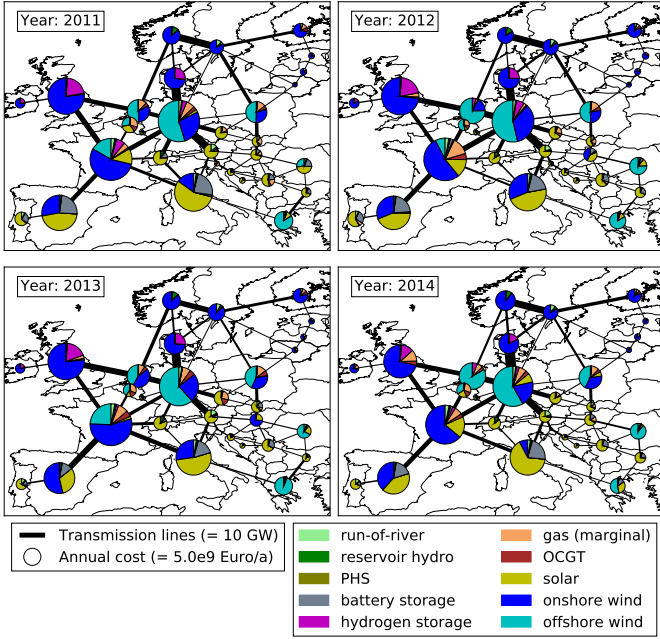


Figure 3: Map of average annual system costs per country in the compromise transmission scenario for the four individual years of weather and demand data 2011 to 2014 (left to right, top to bottom). The area of the circles is proportional to the total costs per country. The modelled international transmission lines are shown as black lines with width proportional to their optimised net transfer capacity [15].

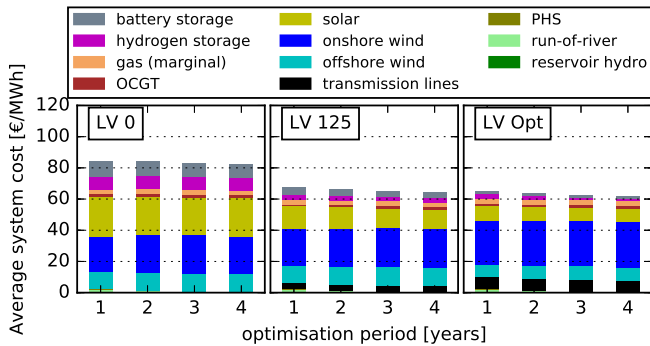


Figure 4: Composition of the average system costs per unit of generated energy for different numbers of simulated weather and consumption years starting from 2011 for the zero, compromise, and optimal (left to right panels) transmission grid scenarios. The color code indicates the contributions of different technologies.

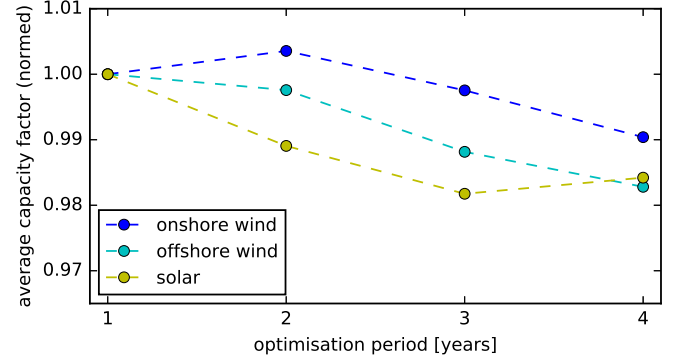


Figure 5: Same as Fig. 2, but for capacity factor cf_s averaged over different numbers of years starting from 2011.

both quantities are significantly smaller, as indicated in Fig. 5.

3h sampling. Some weather data sets, e.g. [34], provide data only in a lower temporal frequency of 3h. Computational restrictions might also prevent an optimisation at a higher temporal resolution, in particular if a very long time frame is considered. At lower temporal resolution, the number of optimisation variables and therefore the memory requirements are proportionately lower and also the computational solving time potentially decreases by a similar magnitude. Both can be limiting factors.

In the following we consider a reduced time resolution by taking 3-hour means of the hourly values of the demand and potential renewable generation time series. The system is then optimised both for the base scenarios year 2011 and the three-year period 2011 to 2013, such that both data sets consider the same number of time steps. Figure 6 shows that the share of solar power slightly increases and replaces wind if the sampling frequency is reduced. This is due to the much stronger fluctuations of solar generation on an hourly timescale compared to wind power generation. The temporal averaging implicitly simulates the smoothing effects of a short term storage, which becomes also apparent in the reduced battery capacity. This effect is not as pronounced in the wind time-series as their dominant fluctuations occur on larger timescales. This indicates that models with time resolution less frequent than one hour might tend to overestimate the effectiveness of solar generation and therefore underestimate battery and wind generation requirements [35, 36, 37, 38]. However, in the scenarios discussed here, the overall effects are small and are in fact outweighed by the fluctuations due to modelling a different period of weather and demand data.

4. Results II: Sensitivity to cost assumptions

Estimates for the future development of costs for technologies that are yet to undergo very large-scale deployment are intrinsically uncertain. In particular solar PV and storage costs could potentially drop significantly over the next decades [32, 39]. Since cost assumptions are a crucial input parameter for

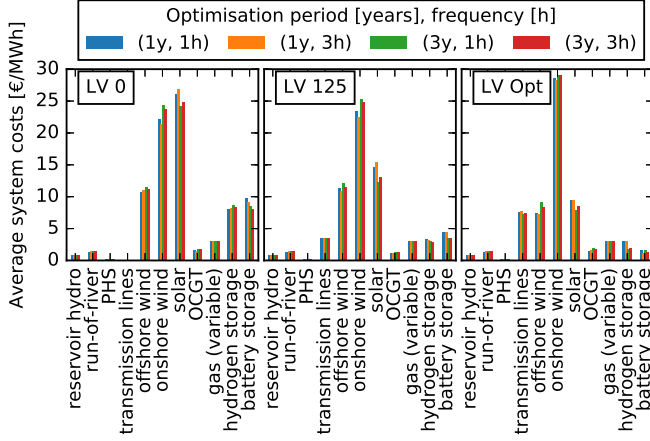


Figure 6: Average system cost of all modelled technologies over total consumption for all four combinations of 1 and 3 simulated years starting from 2011 at 1-hour and 3-hour time resolution (left to right bars) for the zero, compromise, and optimal (left to right panels) transmission grid scenarios. The time resolution was decreased by taking 3-hour means of the hourly values of the demand and potential renewable generation time series.

the optimisation approach in energy system modelling, a comprehensive system analysis has to quantify the sensitivity to cost assumptions in the respective scenarios. This important point is assessed here by varying the capital investment and fixed operation and maintenance cost assumptions for one technology at a time over a large range while keeping all others at their base scenario value.

Solar capital costs. In the base scenario, investment costs for solar PV are assumed to be 600 € per kW of installed capacity. This value is already an extrapolation to the year 2030 and less than half of the cost in 2010, but could be reduced by another 30% until 2050 [32]. In [39] costs for utility-scale PV are foreseen to drop to around 240 €/kW by 2050, which is a drop of 60% compared to the base value.

If the solar capital costs are assumed to be 70% of the base value, or 420 €/kW, for the compromise grid scenario the average total system costs are reduced by 9.6% from 67.5 to 61 €/MWh, as shown in Fig. 7. This reduction of 6.5 €/MWh is slightly larger than the direct cost decrease of 4.4 €/MWh that would occur if only the costs, but not the installed capacity of solar PV are changed. This implies an effective additional benefit to the system due to the shift to a higher solar share from 0.61 TW to 0.87 TW of 2.1 €/MWh, or 3.1% of the total costs when reducing solar costs by 30%.

Even though the total system costs are sensitive to solar cost assumptions, most changes are linear with moderate slopes down to 50%–70% of the solar cost. With decreasing solar costs, the installed capacity, generated energy, and curtailment of wind decrease. It is replaced by additional solar and battery capacity. Additionally, for increasing transmission capacity the power capacity of H₂ storage is almost completely replaced by OCGT capacity (see Fig. 8). This indicates that balancing the demand locally becomes a more dominant solution compared to spatial and long-term smoothing of wind generation, especially

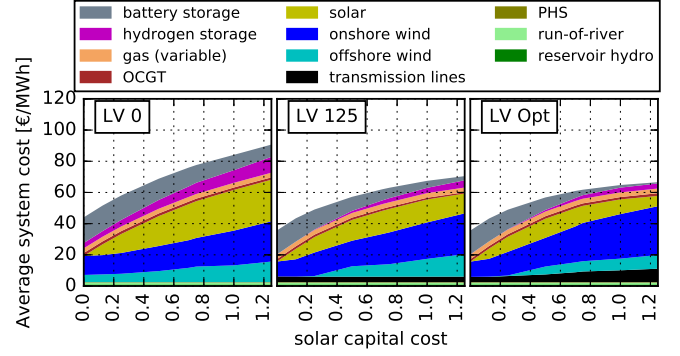


Figure 7: Composition of the average total system costs per unit of generated energy as a function of the fraction of the base solar PV capital cost assumption for the zero, compromise, and optimal (left to right panels) transmission grid scenarios.

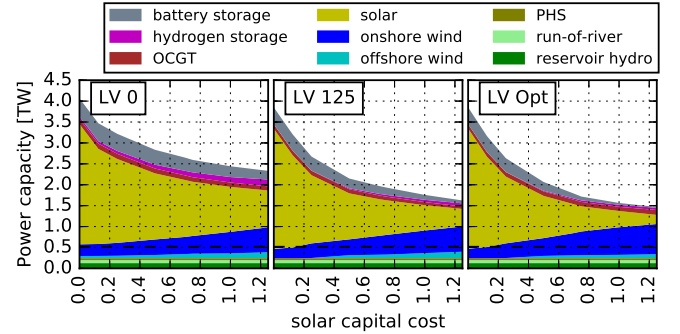


Figure 8: Composition of the total installed power capacity of generators and storage units as a function of the fraction of the base solar PV capital cost assumption for the zero, compromise, and optimal (left to right panels) transmission grid scenarios. The peak of the total demand of 517 GW is marked as a horizontal dashed black line.

in countries with good solar resources. This is also reflected in the transmission volume in the optimal grid scenario, which decreases significantly, but in this range still stays above 125 TWkm, the volume of the compromise grid. A further indication that lower solar costs lead to decentral solutions is the difference between the system costs of the LV 0 and LV Opt scenarios: with the base solar cost, LV 0 is 30% more expensive than LV Opt, but with 70% lower solar cost, LV 0 is only 18% more expensive. In the extreme case that solar generation capacity becomes very cheap compared to the other technologies, even for the optimal grid scenario there is an upper limit of 70% of the consumed energy that can be provided by solar alone, as shown in Fig. 9. However, such a system set-up features huge solar power capacities of up to 2.9 TW, which corresponds to 5.6 times the peak of the total demand. At the same time, a significant amount of solar energy of up to 30% of the yearly consumption has to be curtailed, leading to an inefficient system with a low effective capacity factor. At 40% of the solar cost assumption relative to the base scenario, this technology provides 50% of the energy, with a power capacity of three times the peak of total demand and only a small amount of curtailment. This scenario thus displays a comparatively high

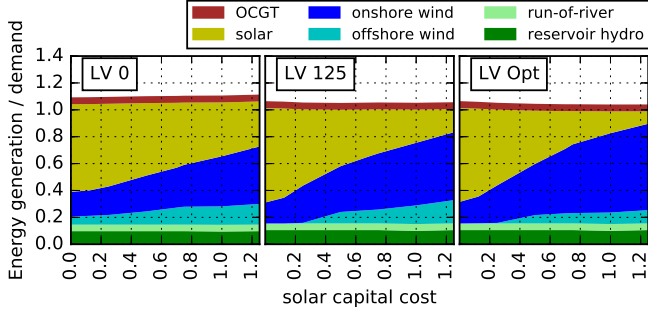


Figure 9: Composition of the total generated energy in units of the total demand as a function of the fraction of the base solar PV capital cost assumption for the zero, compromise, and optimal (left to right panels) transmission grid scenarios. Energy generation above the demand is caused by losses from storage use. The amount of curtailed energy is not shown.

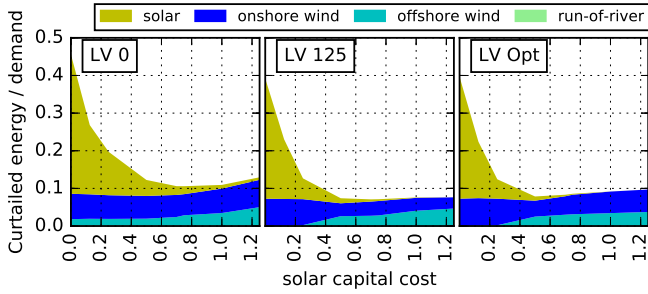


Figure 10: Composition of the total curtailed energy in units of the total demand as a function of the fraction of the base solar PV capital cost assumption for the zero, compromise, and optimal (left to right panels) transmission grid scenarios. The order in which renewables are curtailed is: first offshore wind, then onshore wind, then solar.

efficiency. Figure 10 shows that the amount of curtailed energy remains relatively constant with decreasing solar capital costs at around 8% to 12% of the demand until solar costs are roughly cut in half. Even lower costs lead to the installation of significant overcapacities of solar generation and therefore a strong increase in curtailed energy of up to 40% of the demand. In reality, this overproduction from solar could be used in other energy sectors such as transport and heating, before it is curtailed.

Onshore and offshore wind capital cost. Wind turbines are a mature technology option and have already been deployed on a large scale in recent years, even though there is still significant additional installation potential in Europe. In particular offshore wind turbines are expected to undergo further technological development that will lead to significant cost reductions. Reference [32] assumes a decrease to 1075 and 2093 €/kW by 2050 for onshore wind and offshore wind, respectively, which corresponds to a 9.1% and 16.5% reduction from the 2030 costs.

The optimisation results are already sensitive to moderate changes of the wind cost assumptions. Figure 11 shows that for the compromise grid a 25% reduction of the onshore wind cost decreases the total system costs by 10.4%. While the on-

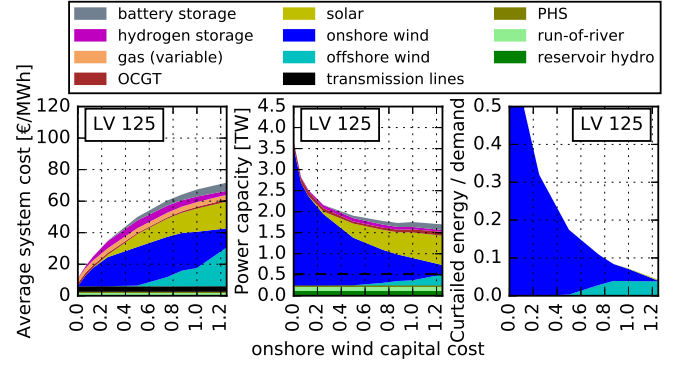


Figure 11: Left: Composition of the average total system costs per unit of generated energy as a function of the fraction of the base onshore wind capital cost assumption. In this figure, all panels are for the compromise transmission grid scenario. Middle: Composition of the total installed power capacity of generators and storage units as a function of the fraction of the base onshore wind capital cost assumption. The peak of the total demand is marked as horizontal dashed black line. Right: Composition of the total curtailed energy in units of the total demand as a function of the fraction of the base onshore wind capital cost assumption. The curtailment at zero cost corresponds to 1.3 times the total demand.

shore wind power capacity increases by 72.9%, half of the offshore wind and a third of the solar installations are no longer required. This higher share of onshore wind generators also leads to a 51.5% increase of the curtailed energy to 10.9% of the total demand. Assuming a less plausible more dramatic decrease of the onshore wind costs, these trends would continue until no offshore wind is built at 50% cost reduction, and almost no solar at 25% of the base scenarios cost assumption. The replacement of the remaining solar capacities is possible with excessive onshore wind power capacity, but would lead to a very large amount of curtailed energy of up to 1.3 times the annual demand. Considering the contrary scenario for a 24% increase of onshore wind costs, up to 42.2% of its installations would be replaced by offshore and solar capacity.

The total system costs are less sensitive to the offshore wind cost assumptions, but still decrease by 7.4% for a 25% lower offshore wind cost for the compromise grid, as shown in Fig. 12. Reducing offshore wind costs leads to a linear increase of its power capacity. It replaces dominantly onshore wind while the solar capacity remains relatively stable and is only slightly decreased. This leads to a significant decrease of the total power capacity by up to 21.3% compared to the base case at a large range of 50% to at least 10% of the assumed cost. At the same time, the amount of curtailed energy remains at or even below the initial value until the offshore wind cost assumptions are halved.

In the limit of very small offshore wind costs, the share of onshore wind is negligible, but solar can still contribute to a cost-optimal system with 241 GW or 14.8% of the total power capacity. This suggests a positive correlation due to a different spatial distribution and the different generation profile of solar. These influences contribute to mitigate line congestions during hours of high demand if large amounts of power have to be transported from remote offshore wind installations.

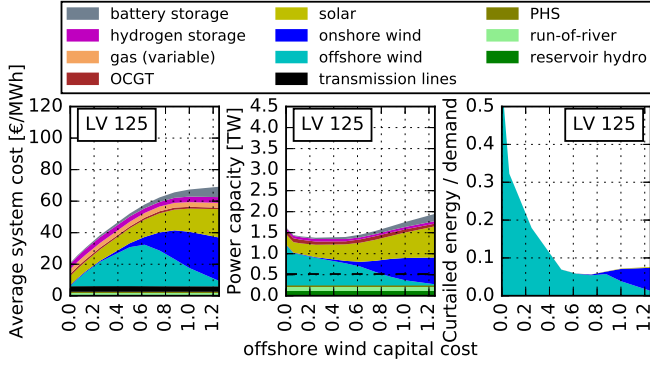


Figure 12: Same as Fig. 11 but as a function of the fraction of the base offshore wind capital cost assumption. The curtailment at zero cost corresponds to 0.57 times the total demand.

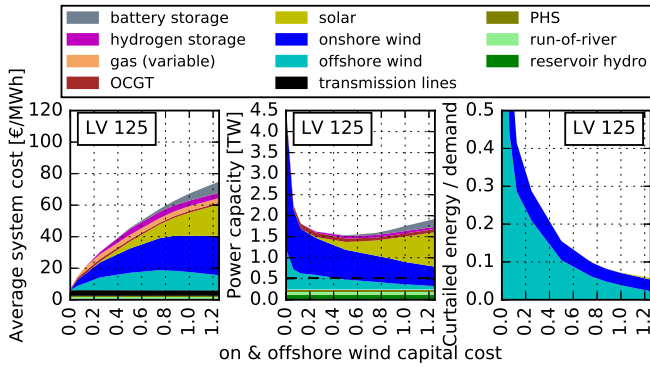


Figure 13: Same as Fig. 11 but as a function of the fraction of both the base onshore wind and the offshore wind capital cost assumption. The curtailment at zero cost corresponds to 2.6 times the total demand.

Figure 13 shows that the system costs decrease even faster than in the previous cases if both the onshore and offshore wind cost assumptions are reduced simultaneously. As in the offshore wind case, the total installed power capacity decreases as the offshore wind installations are expanded and can provide more energy to the system, but a significant amount of solar power is now replaced by an increasing share of onshore wind. For very small cost assumptions, the results are similar to the onshore wind case with additional offshore wind installations that come with even larger amounts of curtailed energy.

Note that even for vanishing solar capital costs, the share of wind power generation in cost optimal configurations does not drop to zero (see Figs. 7 - 10). In contrast, already for moderate transmission expansion for very low onshore capital costs the optimisation leads to a scenario without solar power generation capacity. The fact that it is possible to set up an efficient system without solar, but not without wind power generation shows the value in the European system of the latter, which provides energy at day and night and is seasonally aligned with the peak demand [10].

Battery capital costs. Even though modern battery technology has been commercially available for several decades, their capital costs have dropped significantly over the last few years

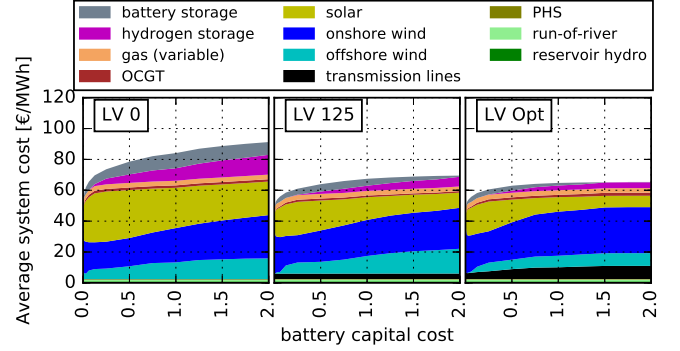


Figure 14: Composition of the average total system costs per unit of generated energy as a function of the fraction of the base battery capital cost for the zero, compromise, and optimal (left to right panels) transmission grid scenarios.

due to technological developments and scaling effects in the manufacturing process [40]. Budischak et al. [6] estimate a price drop by roughly 70% between 2008 and 2030 to values of 310 €/kW for power and 145 €/kWh for energy capacity, as used in the base scenarios.

Since in our model storage power and energy capacity are assumed to be coupled via the technology-dependent time scale $h_{s,max}$ for full charging/discharging, we assume a battery cost reduction which uniformly affects both these cost components. Figure 14 indicates that the modelling results presented here are quite robust against even large changes of battery costs down to 25% relative to the base scenarios assumption. In that case, the total system costs decrease by only 10.6% (7%) to 61 €/MWh (60.6 €/MWh) in the compromise (optimal) grid scenario. Without interconnecting transmission, storage has to provide a large amount of flexibility to ensure system stability. Consequently, the total system costs are more sensitive to the storage costs and decrease by 14.3% to 73.6 €/MWh for the same battery cost change. The installed battery power increases exponentially with decreasing cost from 0.12 TW to 0.41 TW at 25% of the costs (see Fig. 15). However, the solar share increases only linearly at a low rate as more battery capacity becomes available, but stays below 35% of the generated energy. The batteries allow more short-term smoothing and therefore more efficient usage of fluctuating solar generation. This also reduces the required wind capacities, and replaces to a larger extent the more capital intensive offshore wind power. Additionally, the long-term H₂ storage can be completely removed due to a lower wind share and higher solar energy efficiency. The peak demand coverage provided in a few hours per year is then cost-efficiently replaced by additional OCGT power capacity. For very small capital costs, the increase of the total battery power capacity as a function of the cost factor becomes even stronger. This is due to the interaction with onshore wind power. In this limit, the collective battery energy capacity is large enough for long-term storage and allow to smooth out even wind fluctuations over at least several days. Onshore wind is the cheapest renewable generator type in the model in terms of investment costs per average producible energy and can therefore reduce the system costs by replacing solar and offshore wind installa-

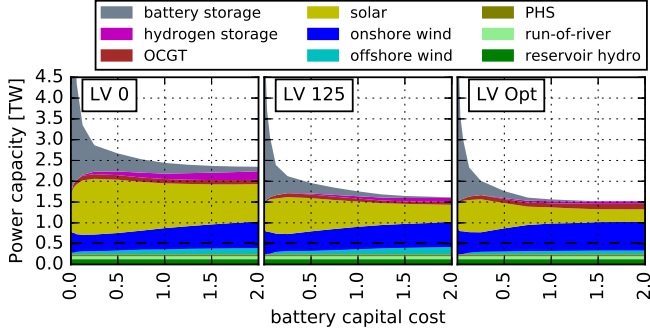


Figure 15: Composition of the total installed power capacity of generators and storage units as a function of the fraction of the base battery capital cost assumption for the zero, compromise, and optimal (left to right panels) transmission grid scenarios. The peak of the total demand of 517 GW is marked as horizontal dashed black line. Recall that the battery energy capacities are given by the power capacities multiplied by the time scale $t_{\text{battery,max}} = 6\text{h}$.

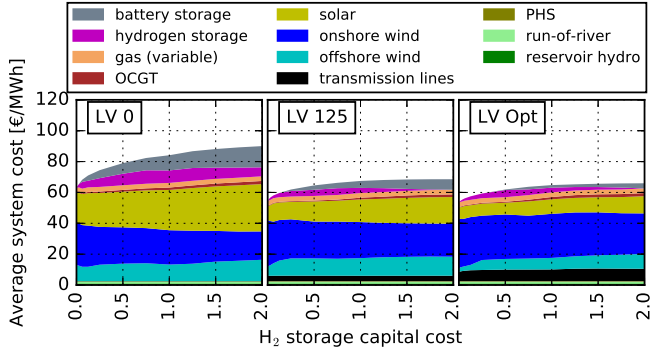


Figure 16: Composition of the average total system costs per unit of generated energy as a function of the fraction of the base H_2 storage capital cost assumption for the zero, compromise, and optimal (left to right panels) transmission grid scenarios.

tions if power balancing is no longer the limiting factor.

Hydrogen storage capital costs. Hydrogen (H_2) storage that is charged by electrolysis of water and discharged via a fuel cell is not yet deployed at a large scale. Its cost and efficiency parameters are characterised by expensive power capacity, but cheap energy capacity with lower round-trip efficiency when compared to battery storage. This makes it adequate for a long-term, large energy storage profile with relatively low usage frequency [6]. Since a commercial large scale implementation is not yet available, large deviations from the base scenario cost assumptions are plausible.

The modelling results are even more robust against changes of the H_2 storage costs than of the battery costs as shown in Fig. 16. Here we have again assumed a uniform decrease in both power and energy capacity of the storage, which are coupled via the time scale $t_{\text{H}_2,\text{max}} = 168\text{h}$. The total system costs correspond closely to the ones in the previous section down to 25% of the base cost assumptions, after which they fall slightly slower with decreasing H_2 storage costs. However, the composition of the system under decreasing H_2 storage costs remains almost identical even for a 75% cost reduction that leads to a

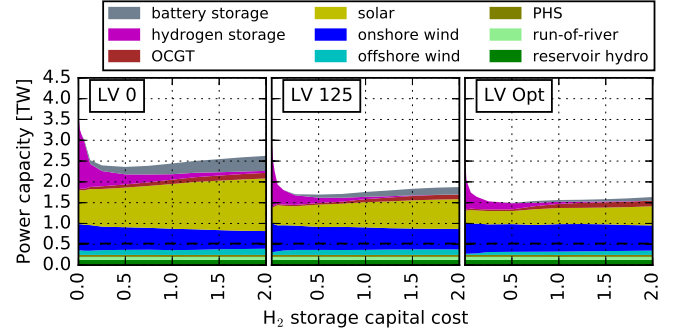


Figure 17: Composition of the total installed power capacity of generators and storage units as a function of the fraction of the H_2 storage capital cost assumption relative to the base scenarios. The peak of the total demand of 517 GW is marked as horizontal dashed black line. Recall that the hydrogen storage energy capacities are given by the power capacities multiplied by the time scale $t_{\text{H}_2,\text{max}} = 168\text{h}$.

capacity increase by a factor of 4.3 in the compromise transmission scenario (see Fig. 17). The share of onshore wind increases only slightly as the H_2 storage cost is lowered. Onshore wind is already the dominant energy source in the system, but can still be made more efficient by additional long-term storage. Simultaneously, some of the solar installations and eventually all battery capacities are removed. Even though the round-trip efficiency of batteries is significantly higher, inexpensive and large H_2 storage capacities, in combination with increased wind installations, provide enough flexibility to the system to even compensate most short-term solar fluctuations.

The installed power capacity of the conventional gas turbines (OCGT) quickly decreases to almost zero already at 80% H_2 costs, but never reaches the limit of zero capacity. The amount of generated energy from this source is determined by the CO_2 emission constraint. The OCGT power capacity decreases because there is sufficiently large H_2 storage capacity which allows to cover all demand peaks mostly from wind energy that previously had to be curtailed but can now be stored in large quantities and over sufficiently long periods. In turn OCGT power does not have to be preserved for extreme hours, but is used by the model as a relatively cheap energy source that is operated almost continuously over the whole year and only shuts down during peak solar production. This maximises the capacity factor of OCGT and avoids most of its capital costs.

If H_2 storage is more expensive than in the base assumption, the previously discussed trends reverse. In this case, H_2 storage is at some point replaced by OCGT, battery, and solar capacity, and is no longer deployed if the costs are increased to more than 175% for both the compromise and the optimum grid scenario. Without transmission, storage is much more important for the security of supply for the system and 36% of the H_2 storage capacity is built even if its cost doubles [15].

5. Results III: Influence of policy constraints

In Ref. [15] the authors investigated the role of different levels of constraints on transmission capacity expansion for cost-

efficient layouts of a European electricity system. The limited geographic potential of different generation and storage technologies as well as a cap on CO₂ emissions entered as fixed constraints into the optimisation. However, for onshore wind a further restriction beyond geographical limits due to public acceptance issues is plausible. In a second investigation different CO₂ caps are implemented, representing less or even more ambitious emission targets than the 95% reduction compared to 1990 levels assumed in the base scenario. The influence of these policy constraints on the system optimisation results are examined.

5.1. Onshore wind potentials

Despite a general positive public attitude towards renewable power generation (in a survey of European Union citizens for the European Commission in 2017, 89% thought it was important for their national government to set targets to increase renewable energy use by 2030 [41]), local onshore wind energy projects appear to be facing increasing opposition throughout Europe [42]. We represent social constraints to the exploitation of onshore wind resources by reducing their maximum installation capacity in each region to a fraction of the geographic potential.

Figure 18 shows the optimisation results for scenarios with such a constrained onshore wind potential. It is found that in this case, onshore wind generation is almost completely replaced by offshore wind. This replacement is not linear with the reduction of onshore wind potential. Some of the onshore installations can be moved to other regions which were not fully using their potentials in the base scenario and have only slightly worse wind conditions. Even though offshore wind turbines have assumed capital costs twice as high as those on land, their average capacity factor is usually much higher (0.485 vs. 0.233 for a layout given by the installation potential $G_{n,s}^{max}$, see Sec. 3) and therefore the average energy generation costs are only slightly higher offshore than onshore. This becomes apparent in the only small increase of total system cost as the amount of onshore wind installation potential is decreased down to zero. The costs change by less than 2.6% if the potential is reduced by half and only up to 8.8-12.2% if no onshore wind is allowed, with the largest increase if transmission is also strongly limited.

Only for strongly reduced potentials do small changes in other parts of the system become visible. Not all countries have access to the sea to build offshore turbines with sufficiently high capacity factors or installation potentials. If transmission capacities are restricted, they have to install slightly more solar PV and batteries, which leads to increasing costs. H₂ storage can be reduced by up to 41% since the feed-in from offshore wind is smoother, but some long term storage is still cost-optimal and the overall cost effect is almost negligible.

The same effects can be observed at country scale as shown in Figs. 19 and 20 for the case with optimal transmission. Onshore wind capacity is replaced by offshore wind in countries bordering the North and Baltic Sea, which is significantly extended in Denmark, the Netherlands, and eventually also in Great Britain. Germany already builds the maximum installable offshore wind capacity in the base scenario and therefore

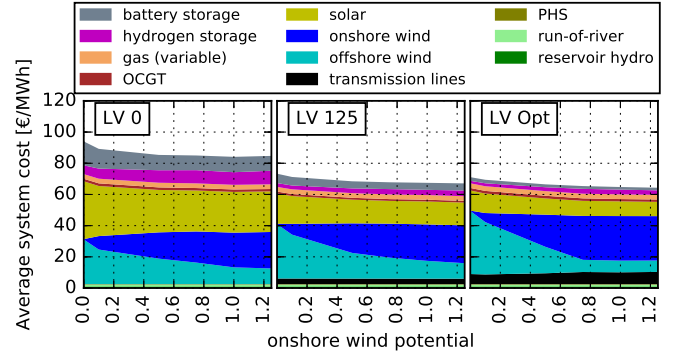


Figure 18: Average total system costs per unit of generated energy in €/MWh as a function of the fraction of the onshore wind potential limit for the transmission line volumes of the zero, compromise, and optimal (left to right panels) grid.

does not replace its onshore wind power. Ireland also does not replace its onshore wind, but simply reduces it. The very large transmission capacities that connect Great Britain and Denmark to their southern neighbors suggest that the energy can now be produced efficiently and without a large grid connection to Ireland in more central nodes of the network. Most countries in the southern half of Europe retain or slightly increase their solar capacity. If no onshore wind is allowed, France installs 45 GW of solar power but no local battery or H₂ storage, while most other countries expand their battery storage together with the solar capacity. This suggests that the solar PV fluctuations in France can be balanced by the more continuous offshore wind generation locally or through imports from the strong grid connection with Great Britain.

The results presented in this study build on a coarse-grained model with each country aggregated to a single node. Onshore potentials and in particular offshore potentials are heterogeneously distributed inside the countries. Corresponding intra-country transmission needs are ignored due to the spatial scale of the model. Nevertheless, since transmission costs represent only a minor component of the total system costs, we expect our results to be stable on a finer scale as long as intra-country transmission can be expanded freely. However, if intra-country capacities are restricted, for example due to public acceptance issues, it may not be possible to integrate all the energy from wind power plants. We refer to the results in [43] and a forthcoming study by the same authors.

5.2. CO₂ emission constraint

Setting a limit to the total European CO₂ emissions is motivated by the policy goal to keep global temperatures from increasing beyond a certain level. In 2011 the European Council reconfirmed the EU objective to reduce overall greenhouse gas emissions by 80-95% compared to 1990 values, including a corresponding emission decrease in the power sector of 93-99% [1]. In the electricity system model applied in the present study, for the base scenario this target is represented as a CO₂ emission limit $CAP_{CO_2} = 5\%$ in units of the emission level

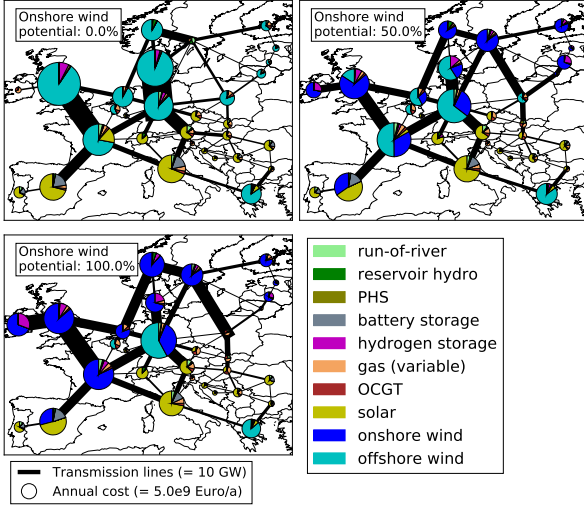


Figure 19: Map of average annual system costs per country in the optimal transmission scenario for three levels of onshore wind potential 0% (top left), 50% (top right), 100% (bottom, base case) of the base assumption in each country. The area of the circles is proportional to the total costs per country. The colors represent the shares of the different technologies. The modelled international transmission lines are shown as black lines with width proportional to their optimized net transfer capacity.

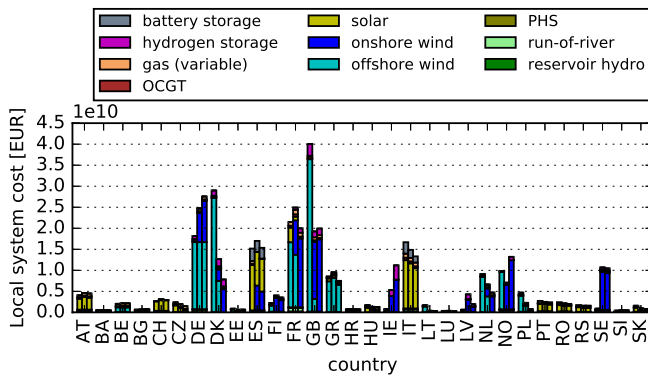


Figure 20: Same data as in Fig. 19 but as a more quantitative bar plot with explicit values of the local system cost and its composition without representation of the transmission lines. The three bars for each country show the level of onshore wind potential 0% (left bar), 50% (middle bar), 100% (right bar), respectively.

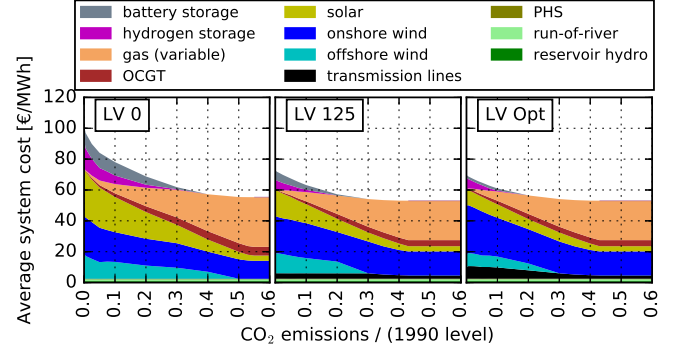


Figure 21: Average total system costs per unit of generated energy as a function of the CO₂ emission limit defined as fraction of the emission level of the year 1990, i.e. 1.55 Gtonne-CO₂, for the zero, compromise, and optimal transmission grid (left to right panels). The base scenarios assume a CO₂ emission level of 5%. For a CO₂ emission level above 30%, the cost-optimal line volume is below 125 TWkm and therefore the compromise and optimal transmission cases are identical.

in the year 1990, i.e., 77.5 Mt-CO₂-equivalent per year for the electricity sector [15, 44].

Going beyond this limit, CO₂ emissions can be brought down to zero by replacing the remaining fossil-fuel based conventional generation. The only conventional generator and source of CO₂ emissions in the model are open-cycle gas turbines (OCGT). This type of generation capacity is highly flexible and has relatively low investment costs for power capacity, but high variable costs for energy generation. This makes this technology option well suited to cover peak residual demand in a few hours per year (see Tab. 2 for the respective cost assumptions).

Figure 21 shows that the total system costs are an almost linear function of the CO₂ emission limit close to $CAP_{CO_2} = 5\%$ with an approximate rate of -0.94 and -0.86 €/MWh per percentage point of CAP_{CO_2} for compromise and optimal transmission volume, respectively. With the compromise (optimal) grid, a system with zero emissions has average system costs of 72 (69) €/MWh, a 6.6% (6.4%) increase from the base scenario.

In the other limit, for an CO₂ emission level above 30%, the transmission system expansion constraint for the compromise grid scenario is no longer binding, i.e. the line volume in the cost-optimal system set-up is below 125 TWkm, leading to identical solutions for both transmission scenarios. The CO₂ constraint in this case is binding up to an emission level of approximately 43%. Since the only emissions in the model result from burning the fuel in the gas turbines, in this range we can directly calculate the corresponding component of the system costs in Fig. 21, using the allowed total CO₂ emissions, the CO₂ emission intensity and efficiency of the gas turbines, and the fuel costs. The gas turbine fuel component of the average system costs is then approximately $CAP_{CO_2} \times 55.39$ €/MWh, with CAP_{CO_2} denoting the CO₂ emission constraint relative to 1990 levels. For $CAP_{CO_2} = 43\%$ or 0.67 Gtonne-CO₂/year this corresponds to 23.82 €/MWh (see Fig. 21).

Once the emission constraint becomes binding, the system optimisation is forced to reduce the amount of energy generated from gas turbines. Figure 21 shows that down to about 20% the

missing energy is then delivered by increasing renewable generation capacity, mostly from solar and offshore wind, while the generation capacity of the gas turbines remains constant. At some point (around 20%/15% for the compromise/optimal grid scenario), the restriction in the usage of the generation from gas turbines starts to affect situations of peaks in the residual load, for which a corresponding increase in renewable generation is no longer a cost-efficient solution. Instead, the system optimisation has to provide the necessary flexibility by a combination of battery and hydrogen storage, which replaces the respective dispatchable power generation also in other situations (see the decrease of gas capacity system costs in Fig. 21). Accordingly, the sum of the installed power capacity of OCGT, battery, and H_2 storage is almost constant at $49 \pm 3\%$ of the peak demand for the compromise grid. Similarly, for the optimal grid the total power of OCGT, battery, H_2 storage, and offshore wind is $52 \pm 2\%$ of peak demand, relatively independent of the emission level. In the latter case, the optimal transmission capacity allows a system-wide usage of the comparatively steady power generation from offshore wind. Nevertheless, the replacement of gas turbines by storage options for stricter emission constraints leads to a stronger increase in system costs, caused by the higher capital costs and reduced efficiencies of these technologies (see Tab. 2 for the respective cost assumptions and efficiencies). Furthermore, the losses associated with using storage technologies represent an additional factor for increasing renewable generation capacities and costs.

Figure 21 shows that the effects of a varying CO_2 emission limit are even more pronounced in the zero transmission scenario. Without transmission the emission constraint becomes binding at $CAP_{CO_2} \approx 53\%$. Power generation from gas is then replaced by generation from larger renewable capacities. At $CAP_{CO_2} < 30\%$, storage units start to replace gas turbines. Transmission not only provides a smoothing effect with respect to the fluctuating renewable generation, but also allows a more efficient system-wide usage of the flexibility provided by storage technologies. Correspondingly, for the zero transmission scenario the total power of OCGT, battery, and H_2 storage increases with a decreasing emission limit. In particular, in the limit $CAP_{CO_2} < 5\%$ both the costs for renewable generators and the storage units grow exponentially.

Open cycle gas turbines are assumed to be the only conventional technology in the system due to their very high flexibility. This assumption starts to break down once conventional generation is no longer needed only for peak load coverage. Today, other conventional technologies, e.g. modern coal power plants, can be more economically efficient if less flexibility and more continuous bulk generation is required. This would lead to a slight reduction of total costs in the extreme case of large CO_2 emission limits. A more thorough analysis of this effect would require detailed modelling of ramping constraints and costs and lies beyond the focus of this work [45].

CO_2 emission shadow price. It should be emphasised that the results above assume a direct CO_2 emission price of 0 €/tonne- CO_2 . Higher prices would lead to smaller economically optimal OCGT shares and emission levels. Fig. 22 plots the shadow

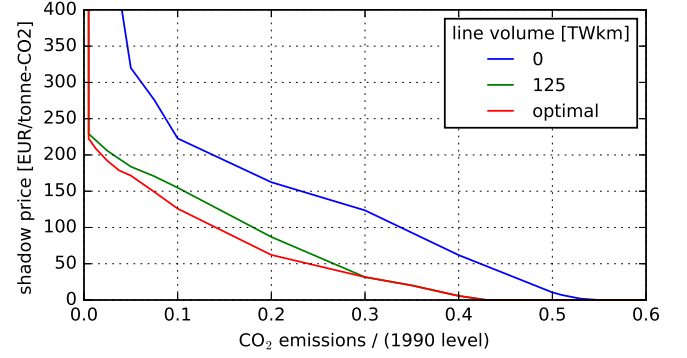


Figure 22: Shadow price of the global CO_2 emission constraint as a function of the CO_2 emission limit CAP_{CO_2} for the zero, compromise, and optimal (blue, green, red lines) transmission scenario. For exactly zero emissions, the shadow price diverges to around 20,000 €/tonne- CO_2 , two orders of magnitude larger than the plotted range. The green and red lines are partly overlapped.

price μ_{CO_2} of the global CO_2 emission constraint in equation (7) against CAP_{CO_2} . Here, μ_{CO_2} can be interpreted as the CO_2 price that would be required for the market to achieve a certain emission level under the given assumptions (for a more general discussion of shadow prices in the context of efficient electricity markets see [46]). A restriction to the $CAP_{CO_2} = 5\%$ level of the base scenario is economically optimal if the emission price is set to roughly 180 €/tonne- CO_2 for both compromise and optimal grid. In these transmission scenarios, the effect of the emission price is similar and the change of μ_{CO_2} with CAP_{CO_2} is close to linear down to very small emission limits. Only if no emissions are allowed, the CO_2 shadow price jumps to around 20000 €/tonne- CO_2 , two orders of magnitude larger than the previous values. This suggests that there is a small number of hours per year when the flexibility provided by the power capacity of OCGT is very valuable for system stability. The system has to install significant additional capacities only to cover the demand in these few hours. In practice, load shedding would be a more viable option for these rare events, but is not included in the model.

The flexibility from the dispatchable generators is much more valuable if fluctuations cannot be smoothed by transmission. In this case, μ_{CO_2} grows at a similar rate with decreasing CO_2 limit as with transmission but is higher by 60 to 100 €/tonne- CO_2 down to $CAP_{CO_2} > 10\%$. For stricter emission limits, μ_{CO_2} increases significantly faster at an exponential rate. $CAP_{CO_2} = 5\%$ can be obtained by an emission price of 319 €/tonne- CO_2 , while $CAP_{CO_2} = 0.5\%$ requires $\mu_{CO_2} = 1280$ €/tonne- CO_2 . This underlines how expensive an ambitious CO_2 reduction is when grid capacity is severely limited.

CO_2 emission constraint without storage. In the previous section it was shown that installing battery and H_2 storage is cost-efficient only if the CO_2 emission limit is very low. In the following the consequences of removing storage altogether are examined, both to understand better the economic necessity of storage and to analyse the case where unforeseen feasibility problems hinder the large-scale deployment of storage.

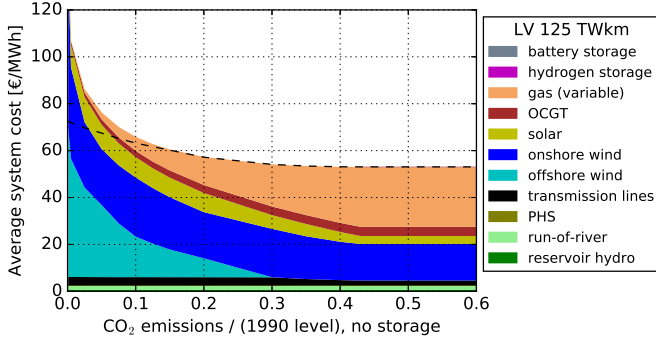


Figure 23: Same as Fig. 21 for the compromise grid but without battery and H₂ storage included in the model. The total system costs for the case including both storage technologies is marked with a black dashed line. For emission levels above 20%, the results are identical to Fig. 21. The optimization did not converge for zero emissions. The smallest computed level of 0.1% has a total cost of 149.6 €/MWh (above plotted range).

Consult Fig. 23 for the cost development as the CO₂ constraint is restricted for the case of moderate transmission expansion (compromise grid scenario). As outlined in the last section, for CO₂ emission reductions to levels above 20%, the results do not differ from the corresponding optimisation including storage. Below 20% the costs rise much faster, being 13.1% higher at 76.3 €/MWh for 5% CO₂, 48.6% higher at 106.9 €/MWh for 0.5% CO₂ and infeasible for 0% CO₂. There is also a significant increase in offshore wind in the range of low CO₂ emissions, as the system optimisation tries to exploit the lower fluctuations of offshore wind to cover the peak residual load. The reason for these strongly increasing costs is the difficulty of bridging times with low wind and sun when there is neither flexibility provided by storage nor gas power generation. Countries must either considerably expand their wind and solar capacities to compensate for the low power availability, or import from other regions where better renewable resource quality provides more generation availability during these times (but even this is restricted by the moderate transmission capacity). The model increasingly introduces offshore wind because of its more regular production characteristics, but as CO₂ emissions are reduced, this is not sufficient to cover the demand at times with strongly adverse weather conditions for wind and solar power generation.

6. Discussion: Limitations of the study

This contribution studies the sensitivity of cost optimal scenarios to various influences for the model presented in Ref. [15]. We explicitly do not extend our investigations to alternative models, which might apply different methodological approaches, incorporate other sectors (like heating and transport) and other technologies (for instance nuclear generation or carbon capture), or consider a finer temporal or spatial scale. This restriction to a single model, for which we have complete knowledge of the underlying data and control over all modelling details, allows us to assess comprehensively the model-inherent sensitivities to input data and optimisation constraints. In contrast,

an inter-model comparison would have to compare scenarios derived from different models for common objectives, without necessarily taking into account the details of the modeling process. For the limitations of the underlying electricity system model we refer to the discussion in Ref. [15].

The strict restriction to one model is applied in Sec. 3, where we study the influence of the sampling in the input load and weather (i.e. renewable generation) time series. Here we choose different samples from the same source and accordingly do not consider alternative sources or modelling frameworks. The load data is at country-level as the spatial scale of the present model is given from the transmission system operators (ENTSO-E), so we can exclude a dependence on the regionalisation of the load data as would be necessary in spatially more detailed system models [43]. Nevertheless, the load data could change both in its profile and volume under an increasing electrification and coupling of other sectors, for instance due a wider use of heat pumps or electric vehicles [47, 48]. In contrast, for the renewable generation potentials we expect both an influence from the underlying weather data source and from the modelling approach used for the conversion from weather to generation time series [25, 49, 50]. Also climate change will have an influence on the structure of future weather conditions [51, 52, 53]. Given the importance of the spatio-temporal renewable generation patterns for a highly renewable electricity system, these topics need to be addressed extensively in future research, but are beyond the scope of the present study.

The influence of cost assumptions is discussed in Sec. 4. In general we only consider a variation of one cost component, whereas the remaining parameters are fixed. For the sensitivity to multi-parameter variations we expect a linear behavior for small changes, i.e. an overlay of the individual system effects. For larger variations, non-linear effects will lead to new cost optimal system configurations. Although an extensive exploration of the whole parameter space is not feasible in the context of a single journal paper, we are confident that we have captured the essential interdependencies already in our single-parameter variation approach.

7. Summary and Conclusions

Models of the electricity system give important insights into how to cost-efficiently combine different technology options in the framework given by the physical, environmental, or societal constraints of the system. Even if the methodological approach and the scope of a model is fixed, the simulation results will depend on the assumptions concerning the input data, input parameters, and constraints inside the model. Using the techno-economic optimisation model for the European electricity system presented in Ref. [15], we have studied the influence of the data sampling in the load and renewable generation time series, and of different cost assumptions for the capital costs of generation and storage technologies. Beyond this analysis, we have shown how different policy constraints, in particular the cap on the CO₂ emission level, affect the structure of the cost optimal scenarios.

We observe that trends in different samples of the load and renewable generation time series are reflected in the details of the simulation results, but only weakly affect the resulting total system costs. A shift from an hourly resolution to a 3 hour sampling in the time series for instance slightly increases the share of solar power generation due to the corresponding smoothing of fluctuations on this time scale.

For moderate changes in the solar capital costs we find a linear relationship to total system costs, with onshore wind power being replaced by additional solar and battery capacity for decreasing solar costs. We observe a comparatively stronger sensitivity to onshore wind capital costs. Given a scenario with moderate transmission expansion, a reduction of onshore wind capital costs by 25% leads to decrease of system costs by 10.4%. In contrast, a reduction of battery or hydrogen storage capital costs only has a very weak effect on the modelling results. All in all we observe that for moderate changes in the cost assumptions, the total system costs tend to be flat in the optimisation space, which indicates a certain degree of freedom to consider additional factors like public acceptance in the choice of cost optimal system layouts. The consideration of constraints in the exploitation of onshore wind potentials leads to similar results. In this case, onshore wind capacity is mostly replaced by offshore wind capacity, with only a small increase in total system costs.

The base scenarios studied in [15] assume a CO₂ emission limit of 5% in terms of 1990 levels as a constraint for the system optimisation. Since open cycle gas turbines are the only source of CO₂ emissions considered in the model, this constraint directly translates into the amount of flexible power generation from natural gas. The simulation results shows that a 5% cap on emissions corresponds to a CO₂ shadow price of 180 €/tonne-CO₂/year for both a scenario with optimal and with moderate transmission expansion. This shadow price indicates the carbon dioxide price necessary to obtain the corresponding reduction in emissions in an unconstrained market. For a scenario without transmission between the European countries the CO₂ shadow price rises to 319 €/tonne-CO₂/year, underlining the benefit of transmission for a low-emission electricity system [15]. We observe that for both grid expansion scenarios the emission limit becomes binding for a 43% reduction compared to 1990s level. Stricter constraints necessarily lead to a decrease in the share of power generated from natural gas, which is replaced by renewable generation from expanded wind and solar generation capacities at slightly increasing system costs. For even lower emissions, storage options replace gas turbines and provide the flexibility to meet peak demand situations in cost optimal scenarios. If such storage options are excluded from the system, total costs rise significantly, and the extreme case of a zero-emission scenario becomes infeasible.

This study addresses the sensitivity to changes in the input parameters and to policy constraints for cost optimal scenarios of a low emission electricity system, highlighting the stability of total system costs and the decisive role of the CO₂ emission constraint. Such an analysis provides an understanding of the mechanisms underlying the cost-efficient combinations of different technologies, thus providing insights beyond a mere

listing of scenarios derived from running extensive simulations. Given the uncertainties and complexities of the energy system, such a perspective should be added also to more detailed system models, assessing the role of the spatio-temporal scales, technology options, or sectors considered in their implementation. Only such a broad methodological approach can provide the robust and comprehensible policy guidelines necessary to facilitate a cost-efficient transition to a low-emission sustainable energy system.

Acknowledgements

The project underlying this report was supported by the German Federal Ministry of Education and Research under grant no. 03SF0472C. Mirko Schäfer is funded by the Carlsberg Foundation Distinguished Postdoctoral Fellowship. David Schlachtberger, Tom Brown and Martin Greiner are partially funded by the RE-INVEST project (Renewable Energy Investment Strategies – A two-dimensional interconnectivity approach), which is supported by Innovation Fund Denmark (6154-00033B). The responsibility for the contents lies with the authors.

References

- [1] European Commission, *A roadmap for moving to a competitive low carbon economy in 2050*, Tech. rep., European Commission (Mar. 2011). URL <http://eur-lex.europa.eu/legal-content/EN/TXT/PDF/?uri=CELEX:52011DC0112&from=EN>
- [2] IRENA, *Renewable Power Generation Costs in 2017*, International Renewable Energy Agency, Abu Dhabi, 2018. URL http://irena.org/-/media/Files/IRENA/Agency/Publication/2018/Jan/IRENA_2017_Power_Costs_2018.pdf
- [3] IRENA, European Commission, *Renewable Energy Prospects for the European Union*, International Renewable Energy Agency, Abu Dhabi, 2018. URL http://www.irena.org/-/media/Files/IRENA/Agency/Publication/2018/Feb/IRENA_REmap_EU_2018.pdf
- [4] M. G. Rasmussen, G. B. Andresen, M. Greiner, Storage and balancing synergies in a fully or highly renewable pan-European power system, *Energy Policy* 51 (2012) 642–651. doi:10.1016/j.enpol.2012.09.009.
- [5] D. Connolly, H. Lund, B. Mathiesen, E. Pican, M. Leahy, The technical and economic implications of integrating fluctuating renewable energy using energy storage, *Renewable Energy* 43 (0) (2012) 47–60. doi:10.1016/j.renene.2011.11.003.
- [6] C. Budischak, D. Sewell, H. Thomson, L. Mach, D. E. Veron, W. Kempton, Cost-minimized combinations of wind power, solar power and electrochemical storage, powering the grid up to 99.9% of the time, *Journal of Power Sources* 225 (2013) 60–74. doi:10.1016/j.jpowsour.2012.09.054.
- [7] F. Fattori, N. Anglani, I. Staffell, S. Pfenninger, High solar photovoltaic penetration in the absence of substantial wind capacity: Storage requirements and effects on capacity adequacy, *Energy* 137 (2017) 193–208. doi:10.1016/j.energy.2017.07.007.
- [8] H. Lund, P. A. Østergaard, D. Connolly, B. V. Mathiesen, Smart energy and smart energy systems, *Energy* 137 (2017) 556–565. doi:10.1016/j.energy.2017.05.123.
- [9] F. Cebulla, T. Naegler, M. Pohl, Electrical energy storage in highly renewable European energy systems: Capacity requirements, spatial distribution, and storage dispatch, *Journal of Energy Storage* 14 (2017) 211–223. doi:10.1016/j.est.2017.10.004.
- [10] G. Czisch, *Szenarien zur zukünftigen Stromversorgung*, Ph.D. thesis, Universität Kassel (2005). URL <http://nbn-resolving.de/urn:nbn:de:hebis:34-200604119596>

- [11] K. Schaber, F. Steinke, T. Hamacher, Transmission grid extensions for the integration of variable renewable energies in Europe: Who benefits where?, *Energy Policy* 43 (2012) 123–135. doi:10.1016/j.enpol.2011.12.040.
- [12] K. Schaber, F. Steinke, P. Mühlich, T. Hamacher, Parametric study of variable renewable energy integration in Europe: Advantages and costs of transmission grid extensions, *Energy Policy* 42 (2012) 498–508. doi:10.1016/j.enpol.2011.12.016.
- [13] R. A. Rodríguez, S. Becker, G. B. Andresen, D. Heide, M. Greiner, Transmission needs across a fully renewable European power system, *Renewable Energy* 63 (2014) 467–476. doi:10.1016/j.renene.2013.10.005.
- [14] Y. Scholz, Renewable energy based electricity supply at low costs - Development of the REMix model and application for Europe, Ph.D. thesis, Universität Stuttgart (2012). doi:10.18419/opus-2015.
- [15] D. Schlachtberger, T. Brown, S. Schramm, M. Greiner, The benefits of cooperation in a highly renewable European electricity network, *Energy* 134 (2017) 469–481. doi:10.1016/j.energy.2017.06.004.
- [16] H. C. Gils, Y. Scholz, T. Pregger, D. Luca de Tena, D. Heide, Integrated modelling of variable renewable energy-based power supply in Europe, *Energy* 123 (2017) 173 – 188. doi:10.1016/j.energy.2017.01.115.
- [17] C. M. Grams, R. Beerli, S. Pfenninger, I. Staffell, H. Wernli, Balancing Europe's wind-power output through spatial deployment informed by weather regimes, *Nature Climate Change* 7 (8) (2017) 557–562. doi:10.1038/NCLIMATE3338.
- [18] E. H. Eriksen, L. J. Schwenk-Nebbe, B. Tranberg, T. Brown, M. Greiner, Optimal heterogeneity in a simplified highly renewable European electricity system, *Energy* 133 (2017) 913–928. doi:10.1016/j.energy.2017.05.170.
- [19] S. Pfenninger, A. Hawkes, J. Keirstead, Energy systems modeling for twenty-first century energy challenges, *Renewable and Sustainable Energy Reviews* 33 (2014) 74–86. doi:10.1016/j.rser.2014.02.003.
- [20] S. Pfenninger, L. Hirth, I. Schlecht, E. Schmid, F. Wiese, T. Brown, C. Davis, M. Gidden, H. Heinrichs, C. Heuberger, S. Hilpert, U. Krien, C. Matke, A. Nebel, R. Morrison, B. Müller, G. Pleßmann, M. Reeg, J. C. Richstein, A. Shivakumar, I. Staffell, T. Tröndle, C. Wingenbach, Opening the black box of energy modelling: Strategies and lessons learned, *Energy Strategy Reviews* 19 (2018) 63–71. doi:10.1016/j.esr.2017.12.002.
- [21] T. Brown, J. Hörsch, D. Schlachtberger, PyPSA: Python for Power System Analysis, *Journal of Open Research Software* 6 (1) (2018) 4. arXiv:1707.09913, doi:10.5334/jors.188.
- [22] D. Heide, L. von Bremen, M. Greiner, C. Hoffmann, M. Speckmann, S. Bofinger, Seasonal optimal mix of wind and solar power in a future, highly renewable Europe, *Renewable Energy* 35 (11) (2010) 2483–2489. doi:10.1016/j.renene.2010.03.012.
- [23] European Transmission System Operators, *Country-specific hourly load data* (2011). URL <https://www.entsoe.eu/data/data-portal/consumption/>
- [24] D. Heide, M. Greiner, L. Von Bremen, C. Hoffmann, Reduced storage and balancing needs in a fully renewable European power system with excess wind and solar power generation, *Renewable Energy* 36 (9) (2011) 2515–2523. doi:10.1016/j.renene.2011.02.009.
- [25] G. B. Andresen, A. A. Søndergaard, M. Greiner, Validation of Danish wind time series from a new global renewable energy atlas for energy system analysis, *Energy* 93 (2015) 1074–1088. doi:10.1016/j.energy.2015.09.071.
- [26] European Environment Agency, *Corine land cover 2006* (2014). URL <https://www.eea.europa.eu/data-and-maps/data/clc-2006-vector-4>
- [27] European Environment Agency, *Natura 2000 data - the European network of protected sites* (2016). URL <http://www.eea.europa.eu/data-and-maps/data/natura-7>
- [28] A. Kies, K. Chattopadhyay, L. von Bremen, E. Lorenz, D. Heinemann, RESTORE 2050 Work Package Report D12: Simulation of renewable feed-in for power system studies., Tech. rep., Carl von Ossietzky Universität Oldenburg, Germany (2016).
- [29] B. Pflüger, F. Sensfuß, G. Schubert, J. Leisentritt, *Tangible ways towards climate protection in the European Union (EU long-term scenarios 2050)*, Tech. rep., Fraunhofer ISI (2011). URL https://www.isi.fraunhofer.de/content/dam/isi/dokumente/ccx/2011/Final_Report_EU-Long-term-scenarios-2050.pdf
- [30] European Transmission System Operators, *Installed Capacity per Production Type in 2015* (2016). URL <https://transparency.entsoe.eu/generation/r2/installedGenerationCapacityAggregation/show>
- [31] D. P. Dee, S. M. Uppala, A. J. Simmons, P. Berrisford, P. Poli, S. Kobayashi, U. Andrae, M. A. Balmaseda, G. Balsamo, P. Bauer, P. Bechtold, A. C. M. Beljaars, L. van de Berg, J. Bidlot, N. Bormann, C. Delsol, R. Dragani, M. Fuentes, A. J. Geer, L. Haimberger, S. B. Healy, H. Hersbach, E. V. Hólm, L. Isaksen, P. Kållberg, M. Köhler, M. Matricardi, A. P. McNally, B. M. Monge-Sanz, J.-J. Morcrette, B.-K. Park, C. Peubey, P. de Rosnay, C. Tavolato, J.-N. Thépaut, F. Vitart, The ERA-Interim reanalysis: configuration and performance of the data assimilation system, *Quarterly Journal of the Royal Meteorological Society* 137 (656) (2011) 553–597. doi:10.1002/qj.828.
- [32] A. Schröder, F. Kunz, J. Meiss, R. Mendelevitch, C. von Hirschhausen, *Current and prospective costs of electricity generation until 2050*, Data Documentation, DIW 68, Deutsches Institut für Wirtschaftsforschung (DIW), Berlin (2013). URL http://www.diw.de/documents/publikationen/73/diw_01.c.424566.de/diw_datadoc_2013-068.pdf
- [33] S. Hagspiel, C. Jägemann, D. Lindenberger, T. Brown, S. Cherevatskiy, E. Tröster, Cost-optimal power system extension under flow-based market coupling, *Energy* 66 (2014) 654–666. doi:10.1016/j.energy.2014.01.025.
- [34] D. Jacob, J. Petersen, B. Eggert, A. Alias, O. B. Christensen, L. M. Bouwer, A. Braun, A. Colette, M. Déqué, G. Georgievski, E. Georgopoulou, A. Gobiet, L. Menut, G. Nikulin, A. Haensler, N. Hempelmann, C. Jones, K. Keuler, S. Kovats, N. Kröner, S. Kotlarski, A. Kriegsmann, E. Martin, E. van Meijgaard, C. Moseley, S. Pfeifer, S. Preuschmann, C. Radermacher, K. Radtke, D. Rechid, M. Rounsevell, P. Samuelsson, S. Somot, J.-F. Soussana, C. Teichmann, R. Valentini, R. Vautard, B. Weber, P. Yiou, EURO-CORDEX: new high-resolution climate change projections for European impact research, *Regional Environmental Change* 14 (2) (2014) 563–578. doi:10.1007/s10113-013-0499-2.
- [35] L. Kotzur, P. Markewitz, M. Robinius, D. Stolten, Impact of different time series aggregation methods on optimal energy system design, *Renewable Energy* 117 (2018) 474–487. doi:10.1016/j.renene.2017.10.017.
- [36] P. Härtel, M. Kristiansen, M. Korpås, Assessing the impact of sampling and clustering techniques on offshore grid expansion planning, *Energy Procedia* 137 (2017) 152–161. doi:10.1016/j.egypro.2017.10.342.
- [37] S. Pfenninger, Dealing with multiple decades of hourly wind and PV time series in energy models: A comparison of methods to reduce time resolution and the planning implications of inter-annual variability, *Applied Energy* 197 (2017) 1–13. doi:10.1016/j.apenergy.2017.03.051.
- [38] R. Green, I. Staffell, N. Vasilakos, Divide and Conquer? k-means clustering of demand data allows rapid and accurate simulations of the British electricity system, *IEEE Transactions on Engineering Management* 61 (2) (2014) 251–260. doi:10.1109/TEM.2013.2284386.
- [39] E. Vartiainen, G. Masson, C. Breyer, *The True Competitiveness of Solar PV: A European Case Study*, Tech. rep., European Technology and Innovation Platform for Photovoltaics (2017). URL http://www.etip-pv.eu/fileadmin/Documents/ETIP_PV_Publications_2017-2018/LCOE_Report_March_2017.pdf
- [40] B. Nykvist, M. Nilsson, Rapidly falling costs of battery packs for electric vehicles, *Nature Climate Change* 5 (4) (2015) 329–332. doi:10.1038/nclimate2564.
- [41] European Commission, *Special Eurobarometer 459 Report: Climate Change*, Tech. rep., European Commission (2017). doi:10.2834/92702.
- [42] G. Ellis, G. Ferraro, The social acceptance of wind energy, JRC Science for Policy Report EUR 28182 EN, The Joint Research Centre (JRC) (2016). doi:10.2789/696070.
- [43] J. Hörsch, T. Brown, The role of spatial scale in joint optimisations of generation and transmission for European highly renewable scenarios,

- in: 2017 14th International Conference on the European Energy Market (EEM), 2017. doi:10.1109/EEM.2017.7982024.
- [44] European Environment Agency, National emissions reported to the UN-FCCC and to the EU Greenhouse Gas Monitoring Mechanism (2017). URL https://www.eea.europa.eu/ds_resolveuid/d2a35821365d4ce09b277ab3a85bf305
- [45] D. Schlachtberger, S. Becker, S. Schramm, M. Greiner, Backup flexibility classes in emerging large-scale renewable electricity systems, Energy Conversion and Management 125 (2016) 336 – 346. doi:10.1016/j.enconman.2016.04.020.
- [46] D. R. Biggar, M. R. Hesamzadeh, The Economics of Electricity Markets, Wiley, 2014.
- [47] N. Gerhardt, D. Böttger, T. Trost, A. Scholz, C. Pape, A.-K. Gerlach, P. Härtel, Analyse eines Europäischen 95% Klimazielszenarios über mehrere Wetterjahre – Teilbericht, Tech. rep., Fraunhofer IWES (2017). URL http://www.energieversorgung-elektromobilitaet.de/includes/reports/Auswertung_7Wetterjahre_95Prozent_FraunhoferIWES.pdf
- [48] T. Brown, D. Schlachtberger, A. Kies, M. Greiner, Synergies of sector coupling and transmission extension in a cost-optimised, highly renewable European energy system (2018). arXiv:1801.05290.
- [49] I. Staffell, S. Pfenninger, Using bias-corrected reanalysis to simulate current and future wind power output, Energy 114 (2016) 1224–1239. doi:10.1016/j.energy.2016.08.068.
- [50] P. Henckes, A. Knaut, F. Obermüller, C. Frank, The benefit of long-term high resolution wind data for electricity system analysis, Energy 143 (2018) 934–942. doi:10.1016/j.energy.2017.10.049.
- [51] D. Hdidouan, I. Staffell, The impact of climate change on the levelised cost of wind energy, Renewable Energy 101 (2017) 575–592. doi:10.1016/j.renene.2016.09.003.
- [52] J. Wohland, M. Meyers, J. Weber, D. Witthaut, More homogeneous wind conditions under strong climate change decrease the potential for interstate balancing of electricity in Europe, Earth System Dynamics 8 (4) (2017) 1047–1060. doi:10.5194/esd-8-1047-2017.
- [53] K. B. Karnauskas, J. K. Lundquist, L. Zhang, Southward shift of the global wind energy resource under high carbon dioxide emissions, Nature Geoscience 11 (1) (2018) 38–43. doi:10.1038/s41561-017-0029-9.